

MESOSCALE SIMULATIONS OF MICROSTRUCTURE AND TEXTURE EVOLUTION DURING DEFORMATION OF COLUMNAR GRAINS

G. Sarma, B. Radhakrishnan, and T. Zacharia

Computer Science and Mathematics Division
Oak Ridge National Laboratory
P.O. Box 2008, Oak Ridge, TN 37831-6359, USA

Abstract

In recent years, microstructure evolution in metals during deformation processing has been modeled at the mesoscale by combining the finite element method to discretize the individual grains with crystal plasticity to provide the constitutive relations. This approach allows the simulations to capture the heterogeneous nature of grain deformations due to interactions with neighboring grains. The application of this approach to study the deformations of columnar grains present in solidification microstructures is described. The microstructures are deformed in simple compression, assuming the easy growth direction of the columnar grains to be parallel to the compression axis in one case, and perpendicular in the other. These deformations are similar to those experienced by the columnar zones of a large cast billet when processed by upsetting and drawing, respectively. The simulations show that there is a significant influence of the initial microstructure orientation relative to the loading axis on the resulting changes in grain shape and orientation.

The submitted manuscript has been authored by a contractor of the U.S. Government under contract No. DE-AC05-00OR22725. Accordingly, the U.S. Government retains a nonexclusive, royalty-free license to publish or reproduce the published form of this contribution, or allow others to do so, for U.S. Government purposes.

Introduction

The use of the finite element method for modeling the deformation of metal polycrystals at the mesoscale has become more widespread with recent advances in computational capabilities [1–3]. Since these models make use of crystal plasticity for characterizing the anisotropic constitutive response of the material, they are capable of modeling the effects of interactions between the different grains at the microstructural length scale. By discretizing the individual grains with many elements, these simulations also capture variations in the deformation within each grain. This approach has also been coupled with a Monte Carlo recrystallization model to study the evolution of the deformation substructure during subsequent annealing [4,5].

The objective of the work presented in this paper is to apply the mesoscale deformation model to microstructures with columnar grains, which are typical in metals after solidification. The microstructures are deformed in simple compression, with the easy growth direction of the columnar grains aligned with the compression axis in one case (similar to upsetting), and perpendicular to the compression axis in another case (similar to drawing). The differences in the evolution of the microstructure and texture for the two cases are characterized using the mesoscale modeling technique.

Since microstructures with columnar grains have the same configuration of grains for any section along the easy growth direction, it could be considered unnecessary to discretize the microstructure along that direction, and limit the finite element model to a single plane. This issue was examined by simulating the compression of the microstructure using 3-d and 2-d discretizations. It was found that the inhomogeneity in the deformation along the easy growth direction can be quite significant, leading to different results from 3-d and 2-d simulations.

Crystal Plasticity Model

Crystal plasticity is used as the basis for modeling the constitutive response of the columnar grains. Elastic strains are neglected, and deformation is assumed to occur by slip dominated plastic flow of the material. A simple power-law relationship is assumed between the resolved shear stress $\tau^{(\alpha)}$ and the rate of shear $\dot{\gamma}^{(\alpha)}$ on each slip system [6]

$$\dot{\gamma}^{(\alpha)} = \dot{\gamma}_0 \left| \frac{\tau^{(\alpha)}}{\hat{\tau}} \right|^{\frac{1}{m}} \text{sign}(\tau^{(\alpha)}), \quad (1)$$

where m is the rate sensitivity parameter, and $\dot{\gamma}_0$ is a reference rate of shearing. The increase in resistance to continued plastic deformation due to interactions among dislocations is approximated through the evolution of the critical resolved shear stress $\hat{\tau}$. The resolved shear stress is the projection of the crystal deviatoric Cauchy stress $\boldsymbol{\sigma}'_c$ on the slip plane and along the slip direction, and is obtained using the Schmid tensor (dyadic product of the slip direction $\mathbf{s}^{(\alpha)}$ and the slip plane normal $\mathbf{n}^{(\alpha)}$ vectors) as,

$$\tau^{(\alpha)} = (\boldsymbol{\sigma}'_c : \mathbf{n}^{(\alpha)}) \cdot \mathbf{s}^{(\alpha)} = \boldsymbol{\sigma}'_c \cdot (\mathbf{n}^{(\alpha)} \otimes \mathbf{s}^{(\alpha)}) = \boldsymbol{\sigma}'_c \cdot \mathbf{T}^{(\alpha)} = \boldsymbol{\sigma}'_c \cdot \mathbf{P}^{(\alpha)}. \quad (2)$$

Here $\mathbf{P}^{(\alpha)}$ is the symmetric portion of the Schmid tensor $\mathbf{T}^{(\alpha)}$, and can be used to express the crystal rate of deformation \mathbf{D}_c as a linear combination of the slip systems shear rates,

$$\mathbf{D}_c = \sum_{\alpha} \dot{\gamma}^{(\alpha)} \mathbf{P}^{(\alpha)}. \quad (3)$$

Eliminating $\dot{\gamma}^{(\alpha)}$ between equations (1) and (3), and substituting equation (2) for $\tau^{(\alpha)}$ provides an expression for the crystal deformation rate,

$$\mathbf{D}_c = \left[\sum_{\alpha} \frac{\dot{\gamma}_0}{\hat{\tau}} \left| \frac{\tau^{(\alpha)}}{\hat{\tau}} \right|^{\frac{1}{m}-1} \mathbf{P}^{(\alpha)} \otimes \mathbf{P}^{(\alpha)} \right] : \boldsymbol{\sigma}'_c = \mathcal{S}_c(\boldsymbol{\sigma}'_c) : \boldsymbol{\sigma}'_c, \quad (4)$$

which can be inverted due to the rate dependent assumption in equation (1). For a given rate of deformation, equation (4) must be solved iteratively to obtain the crystal stress. The solution for the crystal stress also provides the slip system shear rates, which are then used to update the crystal orientation. The rate of rotation $\dot{\mathbf{R}}^*$ is controlled by the difference between the crystal spin \mathbf{W}_c (given by the skew-symmetric part of the crystal velocity gradient) and the plastic spin associated with the slip system shears,

$$\dot{\mathbf{R}}^* = \left(\mathbf{W}_c - \sum_{\alpha} \dot{\gamma}^{(\alpha)} \mathbf{Q}^{(\alpha)} \right) \mathbf{R}^*, \quad (5)$$

where $\mathbf{Q}^{(\alpha)}$ is the skew-symmetric part of the Schmid tensor $\mathbf{T}^{(\alpha)}$. Material work hardening is modeled by prescribing the evolution of the critical resolved shear stress,

$$\dot{\hat{\tau}} = H_0 \left(\frac{\hat{\tau}_s - \hat{\tau}}{\hat{\tau}_s - \hat{\tau}_i} \right) \dot{\gamma}^*, \quad (6)$$

where hardening rate H_0 and initial hardness $\hat{\tau}_i$ are material parameters. $\dot{\gamma}^*$ is a measure of the net shearing rate on all the slip systems ($\sum_{\alpha} |\dot{\gamma}^{(\alpha)}|$). The saturation hardness $\hat{\tau}_s$ based on the current slip system state is given by

$$\hat{\tau}_s = \hat{\tau}_{s0} \left(\frac{\dot{\gamma}^*}{\dot{\gamma}_s} \right)^{m'}, \quad (7)$$

where $\hat{\tau}_{s0}$, $\dot{\gamma}_s$ and m' are material parameters.

Finite Element Formulation

The finite element formulation used in the present study is described in greater detail by Sarma *et al* [1] and is based on the hybrid formulation used by Beaudoin *et al* [7]. The crystal plasticity model outlined above provides the constitutive framework for the material response. Balance laws for equilibrium and conservation of mass are used to set up the system of equations for the boundary value problem. Under the hybrid formulation, the equilibrium statement is written as a balance of tractions at the inter-element boundaries. Weighted residuals are formed on the equilibrium statement and the constitutive relation. A third residual on the conservation of mass (which for the case of incompressible plastic deformation reduces to a divergence-free velocity field) completes the formulation. Interpolation functions are introduced for the nodal velocities, element stress components and the pressure. A proper choice of the shape functions for the stress permits elimination of the stress degrees of freedom at the element level.

The deformation of the microstructure is simulated in incremental fashion, assuming the geometry and material state (crystal orientation and slip system critical resolved shear stress) to be fixed during the plastic strain increment. The resulting system of equations is solved until a converged velocity field is obtained. The material state is then evolved using equations (5) and (6) and the geometry is advanced using a simple Euler update.

Due to the non-linear nature of the crystal constitutive response, which must be developed

at each iterative step in the velocity solution, the formulation using the crystal plasticity model becomes computationally demanding. Use of the hybrid approach leads to introduction of additional degrees of freedom for the crystal stresses, thereby adding to the computational burden associated with the stiffness calculations. The advantage of using this approach is the smoothness in the stress field, due to the enforcement of traction balance at the element interfaces in an approximate sense [7]. In the finite element context, the numerical integration required for computing the stiffness matrix can be performed simultaneously for all elements. The choice of piecewise discontinuous interpolation functions for the stress is a key feature of the formulation, which enables computation of the stiffness matrices in a concurrent fashion for all elements. This feature in turn lends itself to exploitation of parallel computing tools to enable simulations using large three-dimensional discretizations.

While the stiffness computations are relatively straightforward to implement on a parallel architecture, the solution of the resulting system of equations poses a bigger challenge. Since direct solvers are difficult to optimize on a parallel machine, it is advantageous to use an iterative procedure, such as the conjugate gradient method. In this context, enforcing the incompressibility constraint requires special attention, since it degrades the numerical condition of the resulting system of equations. In the current formulation, incompressibility is enforced using a modified consistent penalty approach, which seeks to decouple the solution for the pressure field from the conjugate gradient method [8]. The formulation has been implemented for execution on massively parallel supercomputers using the Message Passing Interface (MPI) [9] to handle the communication of data among processors.

Application to Columnar Microstructures

The formulation described in the previous section has been used to simulate the deformation of microstructures containing columnar grains. These microstructures were generated by taking a planar section from the result of a 3-d Monte Carlo grain growth simulation [10], and repeating the section along its normal direction to build up the columnar grains. The microstructures were discretized using one element for each grid point, resulting in a mesh with 40 eight-node brick elements along each side of a cube. The material was assumed to have fcc crystal structure, deforming on $\{111\}\langle 110\rangle$ slip systems. Material parameters were taken from literature [11], based on fitting the crystal plasticity model to mechanical test data for aluminum, and are listed in Table I. Even though columnar microstructures are not produced during industrial processing of aluminum due to the addition of grain refiners, these parameters were chosen for convenience, and the simulations can be easily extended to metals like nickel and Ni-based alloys that do produce columnar grains in large ingots. The microstructures were deformed in simple compression, with

Table I. Material parameters used in the deformation simulations.

m	$\dot{\gamma}_0$ [s ⁻¹]	H_0 [MPa]	$\hat{\tau}_i$ [MPa]	τ_{s0} [MPa]	$\dot{\gamma}_s$ [s ⁻¹]	m'
0.05	1.0	58.41	27.17	61.80	5.0×10^{10}	0.005

compression normal the +Z axis, and equal amounts of extension along the +X and +Y axes. The other three sides of the mesh were constrained to have zero normal velocity. The normal velocity components of the surface nodes were prescribed such that a nominal unit compressive strain rate was maintained during deformation. A compressive strain increment of 1% was applied during each step, and the deformation was carried out to 50% reduction in height. Two types of columnar microstructures were considered, the first

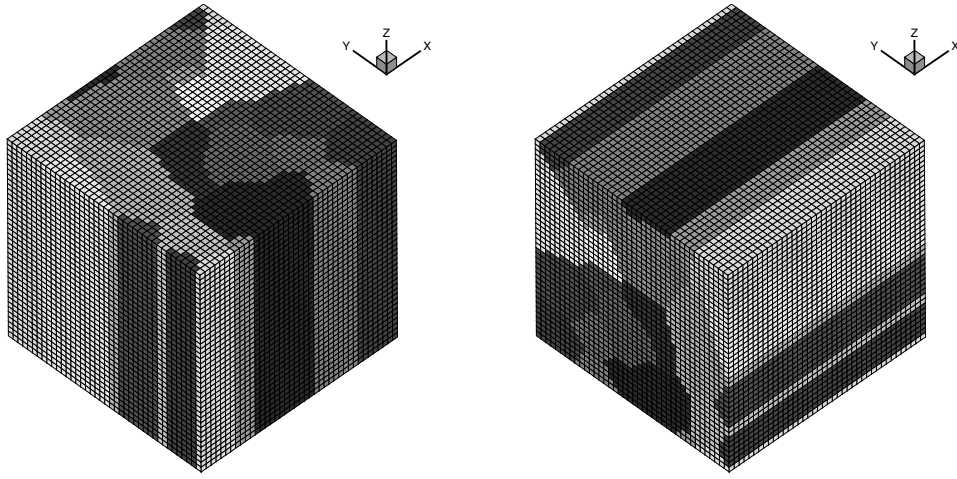


Figure 1: Finite element discretizations of the microstructures with columnar grains aligned with the Z-axis and the X-axis.

with the grains aligned with the Z-axis, and the second with the grains aligned with the X-axis. The initial microstructures and the corresponding finite element discretizations for the two cases are shown in Figure 1. The initial grain orientations for the first case were generated by taking random rotations between $\pm 45^\circ$ about the $[001]$ direction. All elements of a grain were assigned the same initial orientation.

The microstructures shown in Figure 1 were deformed to a compressive true strain of 0.7, and the resulting mesh after deformation for the first case is shown in Figure 2. It is observed that when the columnar grains are aligned with the compression direction, the deformation proceeds fairly uniformly. There is a limited amount of shear in the elements, as observed on the top surface of the deformed 3-d mesh. The grains mostly retain their initial orientations, with only about 5% of the elements developing a misorientation greater than 5° from their initial orientation. This is also evident from Figure 3, which shows the distribution of the $\langle 100 \rangle$ poles shown in equal area projection. The pole figure after deformation was generated using the popLA software package [12], with the application of cubic crystal symmetry and a 5° Gaussian smoothing.

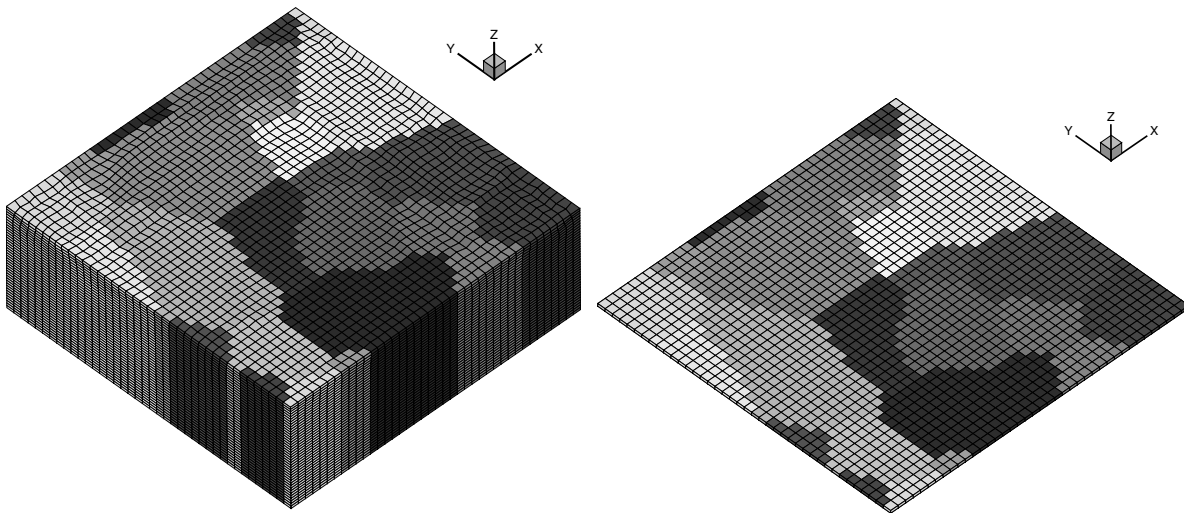


Figure 2: Deformed microstructures with columnar grains aligned with the compression axis obtained using 3-d and 2-d simulations.

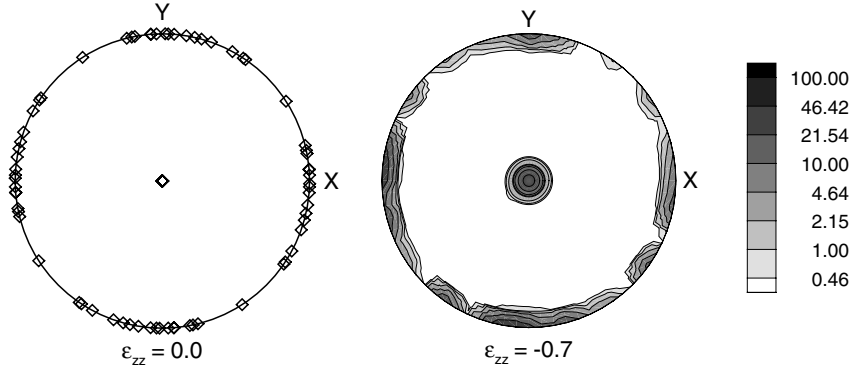


Figure 3: $\langle 100 \rangle$ pole figures in equal area projection showing the initial and deformed textures for the microstructure with columnar grains aligned with the compression axis.

When the grain orientation is such that the $[001]$ direction is perfectly aligned with the compression axis, the crystal plasticity model predicts that a material with fcc crystal structure is able to deform in simple compression with no change in its orientation. This is because of equal shear rates on the complementary slip systems, which cancels out the rotation rate. This has been verified through a calculation using the Taylor mean field hypothesis [13] for grains whose orientations are given by rotations about the $[001]$ direction.

In order to study the effect of the finite element discretization on the deformation of the columnar grains, the same microstructure was also discretized using a mesh with 40×40 eight-node brick elements, which is only one layer thick in the Z-direction. Simulation of simple compression to a strain of 0.7 was carried out similar to the 3-d case, and it was found that all the elements deform uniformly, with no indication of shear in the elements (Figure 2). A plot of the texture showed that the pole figure is identical to that obtained from the initial texture. This result indicates that the reason for small deviations from uniform deformation in the 3-d simulations is the variation from the nominal deformation rate through the thickness of the domain in the compression direction. For the 2-d case, all the nodes are surface nodes, and even though the in-plane velocities of the nodes away from the edges are unconstrained, the simulation proceeds with no deviations from the applied velocity conditions. For the 3-d case, the discretization along the compression direction causes the velocity to develop small deviations from a uniform variation from the top to bottom surface. In turn, this causes the orientations of some elements to evolve differently from their neighbors, thus introducing a slight spread about the initial orientations.

In an effort to further explore the difference between 2-d and 3-d discretizations of columnar microstructures, simulations of the microstructures with columnar grains aligned with the compression axis were repeated, but this time using a different set of initial orientations. These orientations were generated by adding a random perturbation of $\pm 5^\circ$ to each of the three Euler angles from the previous case. Therefore, the initial orientations were not just rotations about the $[001]$ direction, but had an additional small random deviation. The deformed microstructures from the 3-d and 2-d simulations are shown in Figure 4. It is evident that the introduction of small deviations in the initial orientations leads to greater inhomogeneity in the deformation. The 3-d case shows considerable shear in the elements (compare with Figure 2), and the 2-d mesh also shows non-uniform deformation. The resulting textures are shown in Figures 5 and 6, respectively, for the 3-d and 2-d simulations, with significant differences in the pole figures after deformation.

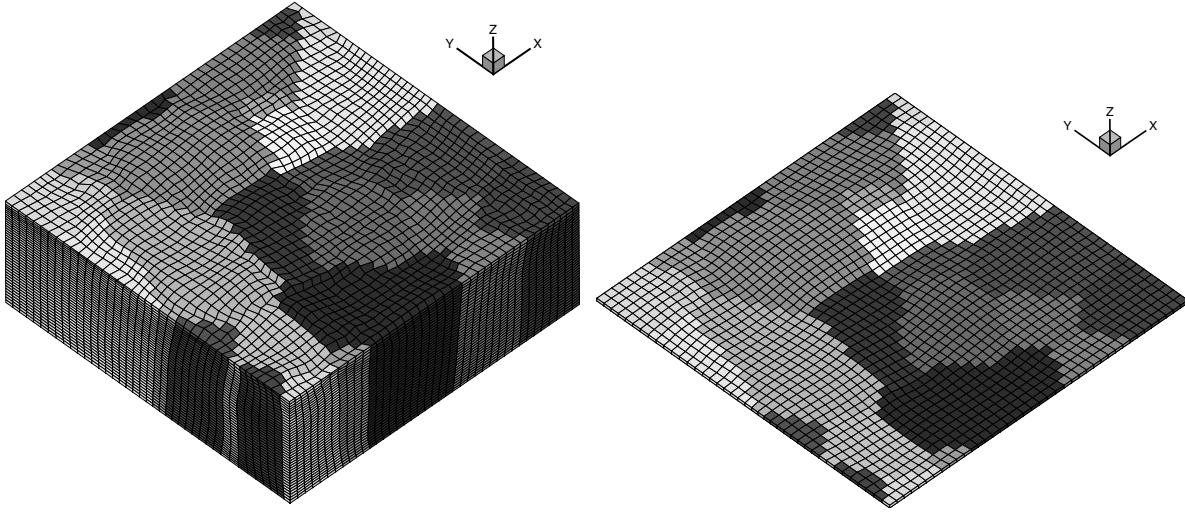


Figure 4: Deformed microstructures with columnar grains aligned with the compression axis with random perturbations in the initial orientations obtained using 3-d and 2-d simulations.

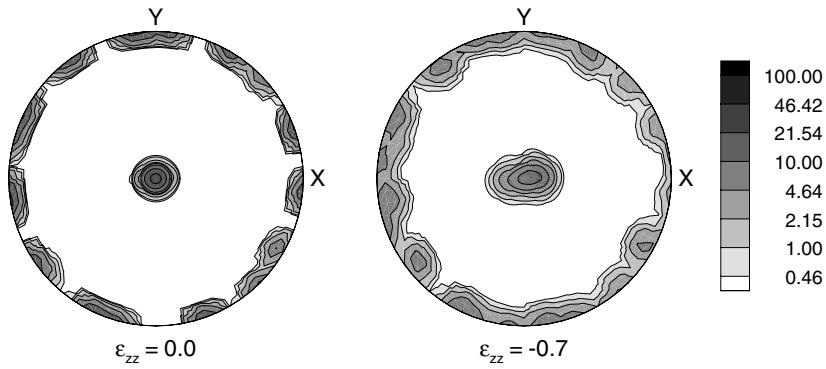


Figure 5: $\langle 100 \rangle$ pole figures from the 3-d simulation showing the initial and deformed textures for columnar grains aligned with the compression axis with random perturbations in the initial orientations.

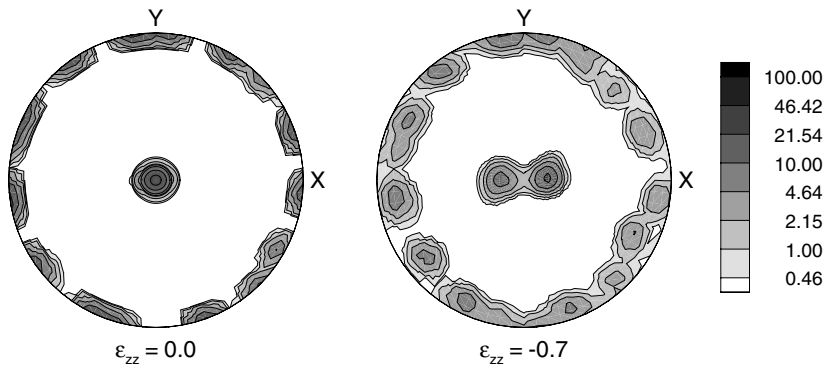


Figure 6: $\langle 100 \rangle$ pole figures from the 2-d simulation showing the initial and deformed textures for columnar grains aligned with the compression axis with random perturbations in the initial orientations.

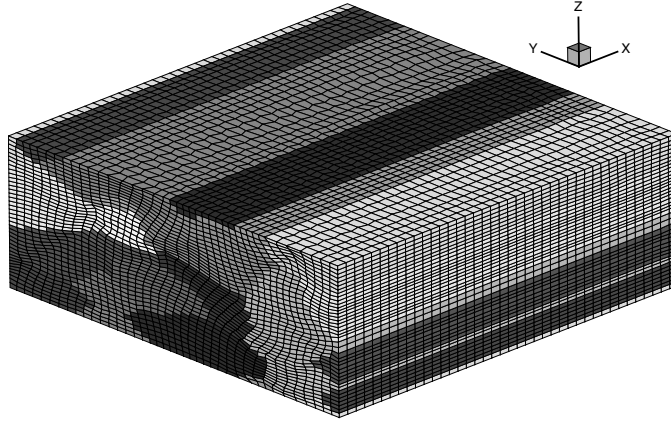


Figure 7: Deformed microstructure with columnar grains perpendicular to the compression axis.

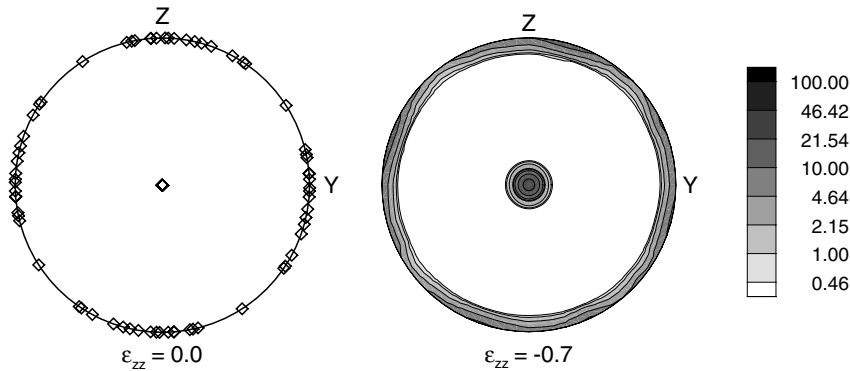


Figure 8: $\langle 100 \rangle$ pole figures in equal area projection showing the initial and deformed textures for the microstructure with columnar grains perpendicular to the compression axis.

The simulation technique described above has also been applied to the case with the columnar grains perpendicular to the compression axis. The same section used in the previous simulations was now repeated along the X-direction to generate the initial microstructure. The finite element mesh was generated as before using 40 elements along each side, as seen in Figure 1. The initial grain orientations were generated by taking random rotations about the $[100]$ direction. The resulting microstructure after compression to 50% reduction in height (true strain of 0.7) is shown in Figure 7. Unlike the earlier case, the deformation of each grain is no longer uniform, and there is considerable shear in certain elements. Most of the elements rotate about the $[100]$ direction by various angles, so that the resulting texture (Figure 8) shows a more or less uniform distribution about this direction.

As in the previous case for grains aligned with the compression axis, the introduction of some random spread in the initial grain orientations leads to greater inhomogeneity in the deformed microstructures. The microstructure after compression to a true strain of 0.7 is shown in Figure 9. In addition to the greater shearing evident in the section normal to the X-axis, there is also greater inhomogeneity along the grain columnar direction. The $\langle 100 \rangle$ pole figures in Figure 10 showing the initial and deformed textures also indicate the influence of the initial spread in the orientations. While the tendency of the grains to rotate about the $[100]$ direction is still present, there is also greater spread in the other directions, with lower peak intensities compared to the previous case.

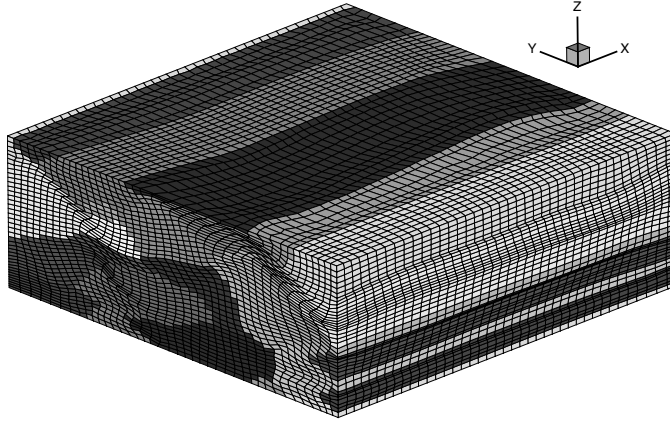


Figure 9: Deformed microstructure with columnar grains perpendicular to the compression axis with random perturbations in the initial orientations.

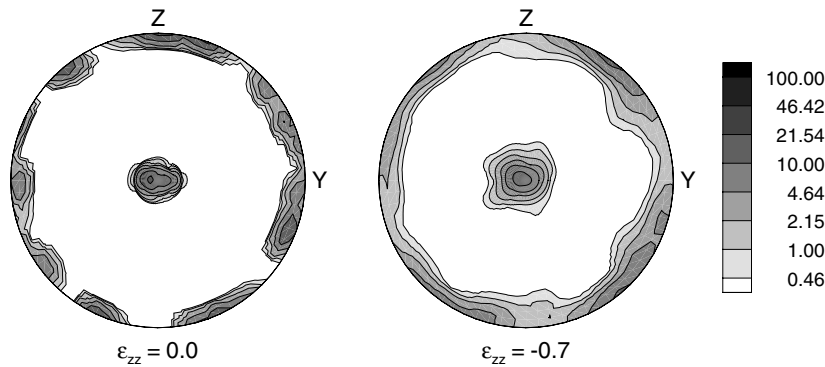


Figure 10: $\langle 100 \rangle$ pole figures from the 3-d simulation showing the initial and deformed textures for columnar grains perpendicular to the compression axis with random perturbations in the initial orientations.

Conclusions

Mesoscale simulations of the deformation of microstructures with columnar grains have been carried out using the finite element method, in conjunction with a crystal plasticity model for characterizing the constitutive behavior. Discretization of the individual grains allowed the simulations to capture the non-uniform deformation of the microstructure due to interactions among the different grains. The simulations showed that the microstructure and texture evolution during simple compression depends on the alignment of the easy growth direction of the columnar grains with the compression axis. This has implications for the upsetting and drawing of billets obtained after casting, since the arrangement of the columnar grains relative to the direction of loading would play a significant role in the resulting microstructure.

A comparison of three-dimensional and planar meshes for simulating the compression of columnar grains showed that the 2-d mesh is unable to capture certain variations in deformation along the grain axis. These variations are greater when the orientations of the columnar grains are not limited to rotations about the easy growth direction, but have additional deviations. The results therefore illustrate the importance of using a three-dimensional discretization in order to better model the inhomogeneous deformations of polycrystal at the mesoscale.

Acknowledgments

This research was sponsored by the Office of Basic Energy Sciences, U.S. Department of Energy, under contract DE-AC05-00OR22725 with UT-Battelle, LLC. This research used resources of the Center for Computational Sciences at Oak Ridge National Laboratory, which is supported by the Office of Science of the U.S. Department of Energy under Contract No. DE-AC05-00OR22725.

References

1. G.B. Sarma, B. Radhakrishnan, and T. Zacharia, "Finite Element Simulations of Cold Deformation at the Mesoscale," Comp Mater Sci., 12 (2) (1998), 105–123.
2. R. Becker, "Modeling of a Columnar Grain Polycrystal Deformed in Plane Strain Compression," Hot Deformation of Aluminum Alloys II (Warrendale, PA: The Minerals, Metals & Materials Society, 1998), 255–266.
3. D.P. Mika and P.R. Dawson, "Polycrystal Plasticity Modeling of Intracrystalline Boundary Textures," Acta Mater. 47 (4) (1999), 1355–1369.
4. B. Radhakrishnan, G. Sarma, and T. Zacharia, "Monte Carlo Simulation of Deformation Substructure Evolution During Recrystallization," Scripta Mater., 39 (12) (1998), 1639–1645.
5. B. Radhakrishnan, G. Sarma, H. Weiland, and P. Beggethun, "Simulations of Deformation and Recrystallization of Single Crystals of Aluminium Containing Hard Particles," Modelling Simul. Mater. Sci. Eng., 8 (5) (2000), 737–750.
6. J. Pan and J.R. Rice, "Rate Sensitivity of Plastic-Flow and Implications For Yield-Surface Vertices," Int. J. Solids Struct. 19 (11) (1983), 973–987.
7. A.J. Beaudoin et al., "A Hybrid Finite Element Formulation for Polycrystal Plasticity with Consideration of Macrostructural and Microstructural Linking," Int. J. Plasticity, 11 (1995), 501–521.
8. A.J. Beaudoin et al., "Application of Polycrystal Plasticity to Sheet Forming," Comput. Meth. Appl. Mech. Engng., 117 (1994), 49–70.
9. Peter S. Pacheco, Parallel Programming with MPI, (San Francisco, CA: Morgan Kaufmann Publishers, Inc., 1997).
10. B. Radhakrishnan and T. Zacharia, "Simulation of Curvature-Driven Grain Growth by Using a Modified Monte-Carlo Algorithm," Metall. Mater. Trans., A26 (1) (1995), 167–180.
11. K.K. Mathur and P.R. Dawson, "On Modeling the Development of Crystallographic Texture in Bulk Forming Processes," Int. J. Plasticity, 5 (1989), 67–94.
12. J.S. Kallend et al., "Operational Texture Analysis," Mater. Sci. Engng. A, 132 (1991), 1–11.
13. G.I. Taylor, "Plastic Strain in Metals," J. Inst. Metals, 62 (1938) 307–324.